COBEM 2021 26th International Congress of Mechanical Engineering
November 22-26, 2021, Virtual Congress, Brazil

COB-2021-0400
MODELING OF MEAN STRESS RELAXATION IN INCONEL 718 UNDER AXIAL-TORSIONAL LOADING AND ITS IMPACT ON FATIGUE LIFE PREDICTION

Vítor Caixeta Fallieri
Fábio Comes de Castro
Cainã Bemfica
Department of Mechanical Engineering, University of Brasilia, 70910-900, Brasilia, DF, Brazil
190136944@aluno.unb.br
fabiocastro@unb.br
cainabemfica@aluno.unb.br

Abstract. *The capability of the Jiang-Sehitoglu plasticity model to describe mean stress relaxation in Inconel 718, and its impact on fatigue life, is studied in this work. To this end, axial-torsional experimental data from Inconel 718 at room temperature is investigated. The model constants were determined from fully reversed and zero-tension axial test data using a nonlinear optimization tool. Half-life mean stresses under proportional and nonproportional loading were simulated and compared with their experimental counterparts to evaluate whether the plasticity model could describe the mean stress relaxation effect. The difference between simulated and observed axial mean stress ranged from -45 to 60% for most loading paths, while for the mean shear stress, the difference ranged from -35 to 35%. For the Chaboche model, which is a particular case of the Jiang–Sehitoglu model, when the exponent of the recovery term is zero, differences ranging from -100 to 65% were noticed for the axial mean stress and -100 to 30% for the mean shear stress. The Fatemi-Socie fatigue criterion was employed to determine the fatigue lives due to the shear cracking behavior of Inconel 718. The implication of considering mean stress relaxation in the fatigue life predictions resulted in life estimation within a factor-of-two boundaries for all loading conditions.*

Keywords: *Inconel 718, mean stress relaxation, axial-torsional fatigue, life prediction.*

1. INTRODUCTION

Inconel 718 is a Ni-based superalloy of widespread use in the aircraft industry. The great value of this material lies in the fact that its mechanical properties are maintained both at low and high temperatures. Since its breakthrough in the late 50's, several studies have been performed aiming to characterize the mechanical behavior of this material. Considering that engineering components made of Alloy 718 usually experience repeated loading, fatigue characterization must be a very well-established parameter for any design. However, fatigue tests are expensive and require varied experimental apparatus to reproduce the different conditions to which components may be subjected. Therefore, computational simulations based on plasticity theories are an alternative way to generate sufficient fatigue data to use this material in safer and more economical applications.

There are many fatigue parameters capable of estimating the fatigue life of various materials. The choice of the parameter to be used will depend mainly on the failure behavior and the stress-strain response of the studied material. Fatigue analysis often uses the stress-strain state referring to half-life hysteresis loops, which is generally the information presented in experimental work. Since the mechanical response will be availed for all cycles with the computational simulations, it is desirable to know what effect the cycle-by-cycle assessment will have on the life estimation. Understanding this behavior is especially important for cases in which the stress-strain response changes along with the cycles, such as when observing the mean stress relaxation phenomenon.

The goal of this study is to simulate the mean stress relaxation effect on Inconel 718, also assessing its influence on fatigue life prediction under axial-torsional loading conditions. To this end, two plasticity models were considered to simulate the stress-strain response of different loading paths: the Jiang-Sehitoglu (J-S) and the Chaboche models. The difference between the two models lies in the fact the former includes an extra variable that controls the ratchetting/mean stress relaxation rate. The calibration of the models was carried out with a nonlinear optimization tool using zero-tension and fully reversed axial test data. The effectiveness of each model in describing the half-life mean stress was evaluated from experimental data of several axial-torsional loading paths. A comparison between experimental and simulated fatigue lives based on the Fatemi and Socie (1988) criterion was made using the stress-strain behavior simulated with both models.

2. METHOD FOR FATIGUE LIFE PREDICTION

Methods for fatigue life prediction are usually based on four components (Socie and Marquis, 2000): a constitutive model for the calculation of the cyclic stress-strain response, a fatigue damage parameter, a cycle counting method, and a damage accumulation rule. The modeling approaches adopted for each of these four components are presented in this section.

The simulation of the stress-strain response was performed using a framework based on the rate- and temperature-independent cyclic plasticity theory described by Chaboche (1986). The total strain is decomposed into a sum of elastic and plastic components. The elastic behavior is described by the generalized Hooke's law, while the plastic strain rate is associated with a von Mises yield surface which is only allowed to translate, indicating that no isotropic hardening is considered. These conditions are expressed as:

$$\boldsymbol{\varepsilon} = \boldsymbol{\varepsilon}^p + \boldsymbol{\varepsilon}^e, \tag{1}$$

$$\boldsymbol{\sigma} = \mathbb{C}\boldsymbol{\varepsilon}^e, \tag{2}$$

$$f = \|\mathbf{S} - \boldsymbol{\alpha}\|^2 - 2k^2, \tag{3}$$

$$\dot{\boldsymbol{\varepsilon}}^p = \dot{\lambda}\frac{\partial f}{\partial \boldsymbol{\sigma}}, \tag{4}$$

where $\boldsymbol{\varepsilon}$, $\boldsymbol{\varepsilon}^e$ and $\boldsymbol{\varepsilon}^p$ are the total, elastic, and plastic strain tensors, respectively; $\boldsymbol{\sigma}$ and $\mathbb{C}$ are the Cauchy stress and isotropic elasticity tensors, respectively; $\mathbf{S}$ and $\boldsymbol{\alpha}$ are the deviatoric stress and backstress tensors, respectively, and k is the cyclic yield stress in simple shear; $\dot{\lambda}$ is the equivalent plastic strain rate, defined as $\|\dot{\boldsymbol{\varepsilon}}^p\|$.

The backstress tensor $\boldsymbol{\alpha}$ associated with kinematic hardening is the center of the yield surface and can be decomposed into M parts as expressed in Eq. (5) (Chaboche et. al, 1979). Based on the model developed by Armstrong and Frederick (1966), Jiang and Sehitoglu (1996a) proposed a hardening rule (Eq. (6)) aiming to describe the mean stress variation behavior over proportional and non-proportional loadings.

$$\boldsymbol{\alpha} = \sum_{i=1}^{M} \boldsymbol{\alpha}^{(i)}, \tag{5}$$

$$\dot{\boldsymbol{\alpha}}^{(i)} = c^{(i)} r^{(i)} \left[\boldsymbol{N} - \left(\frac{\|\boldsymbol{\alpha}^{(i)}\|}{r^{(i)}} \right)^{\chi^{(i)}} \frac{\boldsymbol{\alpha}^{(i)}}{\|\boldsymbol{\alpha}^{(i)}\|} \right] \dot{p}, \tag{6}$$

where $c^{(i)}$, $r^{(i)}$, and $\chi^{(i)}$ are material parameters that, in general, are sets of non-negative and single-valued scalar functions; $\boldsymbol{N}$ is the unit normal to the yield surface; $\dot{p} = \|\dot{\boldsymbol{\varepsilon}}^p\|$ is the equivalent plastic strain rate. Material parameter $r^{(i)}$ can be understood as the radius of the von Mises-type surface. It is interesting to observe that when $\chi^{(i)} = 0$ $(i = 1,2,\dots,M)$, Eq. (6) delivers the Chaboche model: $\dot{\boldsymbol{\alpha}}^{(i)} = c^{(i)}\left(r^{(i)}\boldsymbol{\varepsilon}^p - \boldsymbol{\alpha}^{(i)}\dot{p}\right)$ (Chaboche et. al, 1979). The difference between these models lies in the fact that the Jiang-Sehitoglu model can simulate situations that do not result in total mean stress relaxation, justifying the choice of this model to evaluate the impact of the mean stress in life prediction.

A fatigue criterion consistent with the failure mechanism of Inconel 718 should be used to estimate fatigue life. Socie (1987) observed that Inconel 718 exhibits mode II shear cracks in tension and torsion loading. This observation suggests that the fatigue life prediction model proposed by Fatemi and Socie (1988) (F-S) should be employed for this material. F-S is a fatigue model based on the critical plane approach and considers that fatigue cracks initiate and grow on planes where the shear strain amplitude reaches the maximum values. Among the planes considered, the critical plane that results in final failure will be the one where the maximum normal stress is observed. Life estimates can be obtained using the Coffin-Mason relation. The fatigue parameter proposed by F-S is shown in Eq. (7) on the left side, while the Coffin-Manson relation is shown on the right side.

$$\frac{\Delta\gamma_{max}}{2}\left(1 + K\frac{\sigma_{n\,max}}{\sigma_Y}\right) = \frac{\tau_f'}{G}\left(2N_f\right)^{b_0} + \gamma_f'\left(2N_f\right)^{c_0}, \tag{7}$$

where γ_{max} and $\sigma_{n\,max}$ are the maximum shear strain and normal stress on the plane of maximum shear strain amplitude, respectively, σ_Y is the yield strength of the material, G is the shear modulus, N_f is the number of cycles to failure, and K, τ_f', b_0, γ_f' and c_0 are material constants determined after fitting uniaxial data against pure torsion data. This model accounts for mean stress effects through the normal stress term, which was normalized by the yield strength to keep the parameter dimensionless. To considerer the mean stress relaxation effect on the life prediction approach, a damage model was used to determine the damage increment ΔD per cycle. Failure will occur when the sum of the damage increments is equal to 1, that is,

$$\Delta D = \frac{1}{N_f}, \tag{8}$$

$$D = \sum_{i=1}^{N_{pred}} \Delta D = 1, \tag{9}$$

where N_{pred} is the predicted fatigue life.

3. DETERMINATION OF MATERIAL CONSTANTS

Material constants of the Jiang and Sehitoglu model were obtained from a computational optimization process to solve a minimization problem. This process aimed to determine the constants k, $c^{(i)}$, $r^{(i)}$, and $\chi^{(i)}$ that minimize the difference between simulated and experimental values of the mean and alternate stresses. Room temperature fatigue data for Inconel 718 under fully-reversed and zero-tension axial tests obtained by Socie and Shield (1984), Socie et al. (1985), and Socie et al. (1989) were used to calibrate the J-S model. The basic mechanical properties of this material are: Young's modulus E = 209 GPa, shear modulus G = 78 GPa, yield stress σ_Y = 1160 MPa, and Poisson's ratio ν = 0.3. The initial strategy was to keep the values of $\chi^{(i)}$ equal while varying all other constants. However, this approach was not effective. According to Jiang and Sehitoglu (1996b), the material constants of the hardening rule of the J-S model can be divided into two groups: the first include constants $c^{(i)}$ and $r^{(i)}$, and characterizes cases when no mean stress relaxation and/or ratchetting is observed on a material initially isotropic; the latter is represented by constants $\chi^{(i)}$ and describes mainly loadings that produce mean stress relaxation and/or strain ratchetting on an initially isotropic material. Therefore, it can be concluded that the mean stress relaxation effect simulated by this model is strongly influenced by constants $\chi^{(i)}$.

An objective function Φ was proposed to determine the material constants of the J-S parameter. This function aimed to minimize the square difference between the simulated and experimental alternate and mean stresses obtained from different fatigue tests. Each of these differences was normalized by the corresponding maximum alternate or mean stress obtained from fatigue test data in the literature. The objective function results from the sum of the terms generated from the mean and alternate stresses of all fatigue tests considered during the calibration. The set of constants that calibrate the J-S model are the ones that minimize the objective function. Equation (10) describes the objective function proposed.

$$\min \Phi(\boldsymbol{x}) = \sum_{j=1}^{n_c} \left[\frac{\left(\sigma_{m_s}^{(j)}(\boldsymbol{x}) - \sigma_{m_e}^{(j)}\right)}{\sigma_{m_{max}}}\right]^2 + \left[\frac{\left(\sigma_{a_s}^{(j)}(\boldsymbol{x}) - \sigma_{a_e}^{(j)}\right)}{\sigma_{a_{max}}}\right]^2, \tag{10}$$

where $\boldsymbol{x} = [k,\ c^1\ \ldots\ c^M,\ r^1\ \ldots\ r^M,\ \chi^1\ \ldots\ \chi^M]$ is a vector containing all the constants to be optimized; n_c is the number of fatigue tests used to calibrate the model; σ_{m_s} and σ_{a_s} are the mean stress and stress amplitude simulated from the J-S model; σ_{m_e} and σ_{a_e} are the experimental mean stress and stress amplitude obtained from literature fatigue data of Inconel 718; $\sigma_{m_{max}}$ and $\sigma_{a_{max}}$ are the maximum mean and alternate stresses observed on the literature database considered. All stresses, both experimental and simulated, were obtained at half-life.

Strain-controlled axial-torsion fatigue testing with thin-walled tubular specimens was evaluated in this work. The fatigue tests considered for the calibration of the J-S model were the fully reversed and zero-tension axial tests carried out by Socie and Shield (1984), Socie et al. (1985), and Socie et al. (1989). For such experimental configurations, the axial and/or shear stress distributions can be assumed uniformly distributed over the cross-section of the specimen. By taking advantage of this feature, the numerical implementation of the cyclic plasticity model was achieved by developing a MATLAB script that simulates the stress response of a material point under prescribed axial and shear strains. For each loading condition, the stress amplitude and mean stress at half-life were simulated using the Implicit Euler method. The objective function was then solved by a built-in MATLAB function called "*lsqnonlin*", which is based on the trust-region-reflective algorithm. The initial set of constants was obtained using the method proposed by Jiang and Sehitoglu (1996b). The results of the optimization process are shown in Table 1, where the initial and optimized set of constants are presented ($M = 5$).

Table 1. Initial and optimized set of constants of the J-S model.

Constants	Initial	Optimized
k	462	423
$c^{(i)}$	[2206, 636, 203, 70, 26]	[3708, 1070, 341, 118, 44]
$r^{(i)}$	[39, 61, 61, 61, 104]	[57, 90, 90, 90, 153]
$\chi^{(i)}$	[5, 5, 5, 5, 5]	[101, 297, 232, 24, 5]

Material constants for the FS model were obtained from the experimental data from Socie et al. (1989). Fully reversed pure torsion fatigue results were used to determine the material constants from the Coffin-Manson relation. The procedure used to calibrate the F-S criterion resulted in the following constants: fatigue strength coefficient τ_f' = 2237 MPa, fatigue strength exponent b_0 = -0.16, fatigue ductility coefficient γ_f' = 10.3, and fatigue ductility exponent b_0 = -0.93. The constant K of the F-S parameter was obtained by minimizing the logarithmic difference between the estimated and the experimental fatigue lives. Using pure axial and torsional data from fully reversed fatigue tests, it was concluded that a K = 0.56 resulted in the best fit. This calibration can be observed in Figure 1, where all experimental data were within a factor of 2.

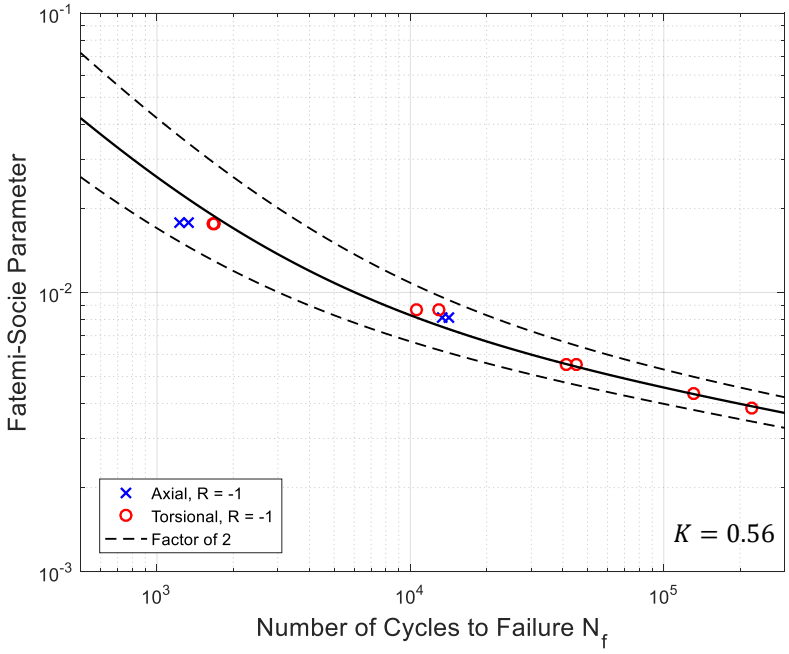

Figure 1. Calibration of the F-S parameter.

4. RESULTS AND DISCUSSION

Socie et al. (1989) reported the experimental half-life stress-strain behavior of Inconel 718 and its fatigue lives N_f^{exp} for fifteen different loading conditions (A - O). All these loading paths are illustrated in Figure 2. The same loading conditions considered in Socie's work were used to assess the capability of the Jiang-Sehitoglu model in simulating the stress-strain response of this material. The fatigue life predictions were accomplished with the Fatemi-Socie parameter. The results of the simulations, which include the half-life stresses (σ_a^{JS}, σ_m^{JS}, τ_a^{JS}, τ_m^{JS}) and the fatigue life prediction (N_f^{JS}), are presented in Table 2. The replica of no case was represented in this table, considering that the simulated stresses would be the same. Among the loading paths tested, proportional and non-proportional loading conditions were considered, including out-of-phase paths. For comparison purposes, life prediction was also obtained using the stress-strain response simulated by the Chaboche model. For this model, constants presented in Table 1 were also used, with the exception of χ, which became a null vector. The simulated Chaboche stress-strain response at half-life returned null values for the mean axial and shear stresses, due to total mean stress relaxation effect, an expected characteristic of this model. The comparison between experimental and simulated half-life stresses is shown in Figure 3 for the J-S and the Chaboche models. The comparison was performed using a percentage difference parameter PD that divides the difference between the simulated and experimental stresses by the respective experimental stress. For cases where null experimental stresses or strains were observed, the PD parameter was calculated using as a divisor the respective maximum stress finds on the literature database considered. Moreover, the fatigue lives predicted from the simulations made with the Chaboche model, N_f^C, are also presented in Table 2.

Table 2. Stress-strain response and life prediction of Inconel 718 simulated with J-S and F-S models

Path	Test No.	ε_a [%]	ε_m [%]	γ_a [%]	γ_m [%]	β [°]	σ_a^{JS} [MPa]	σ_m^{JS} [MPa]	τ_a^{JS} [MPa]	τ_m^{JS} [MPa]	N_f^{JS} [cycles]	N_f^{C} [cycles]	N_f^{exp} [cycles]
A	2	1.00	0.00	0.00	0.00	-	1141	0	0	0	893	897	1050
	3	0.50	0.50	0.00	0.00	-	926	0	0	0	5115	5135	13500
B	6	0.00	0.00	1.76	0.00	-	0	0	671	0	872	875	800
	7	0.00	0.00	0.87	0.00	-	0	0	566	0	3999	4011	7200
	9	0.00	0.00	0.54	0.00	-	0	0	431	0	21096	21097	34000
	11	0.00	0.00	0.43	0.00	-	0	0	346	0	63225	63225	105000
	12	0.00	0.00	0.38	0.00	-	0	0	305	0	123328	123328	114000
C	14	0.71	0.00	1.23	0.00	0	792	0	482	0	798	801	1200
	16	0.35	0.00	0.61	0.00	0	633	0	415	0	3929	3961	7000
	17	0.15	0.00	0.27	0.00	0	314	0	217	0	172586	172586	160000
D	20	1.00	1.00	0.00	0.00	-	1141	26	0	0	882	897	800
	21	0.50	0.50	0.00	0.00	-	926	203	0	0	4499	5134	7000
E	23	0.00	0.00	1.73	1.73	-	0	0	669	3	897	902	1000
	25	0.00	0.00	0.87	0.87	-	0	0	566	89	3891	4011	4500
F	28	0.71	0.71	1.23	1.23	0	792	10	482	3	791	801	1000
	29	0.35	0.35	0.63	0.63	0	628	120	424	71	3413	3756	4800
G	31	0.35	-0.35	0.63	-0.63	0	628	-115	424	-68	4047	3757	6000
H	33	0.35	0.00	0.63	0.63	0	628	-13	424	89	3477	3756	5000
I	35	0.35	0.00	0.63	0.63	180	628	13	424	89	3539	3757	4000
J	37	0.35	0.35	0.63	0.00	0	628	153	424	-7	3229	3757	3000
K	40	0.00	0.10	0.86	0.00	-	0	54	565	0	3867	4141	7470
	41	0.00	0.15	0.38	0.00	-	0	314	305	0	60170	60170	52000
L	43	0.00	-0.10	0.86	0.00	-	0	-54	565	0	4131	4141	9090
	44	0.00	-0.15	0.38	0.00	-	0	-314	305	0	124285	124285	462000
M	45	0.35	0.00	0.62	0.00	45	679	0	444	0	3899	3873	5550
N	47	0.71	0.00	1.23	0.00	90	1018	0	600	0	874	866	430
	49	0.35	0.00	0.62	0.00	90	734	0	472	0	4811	4776	4370
O	51	0.35	0.35	0.62	0.00	90	734	230	472	0	3868	4775	3550

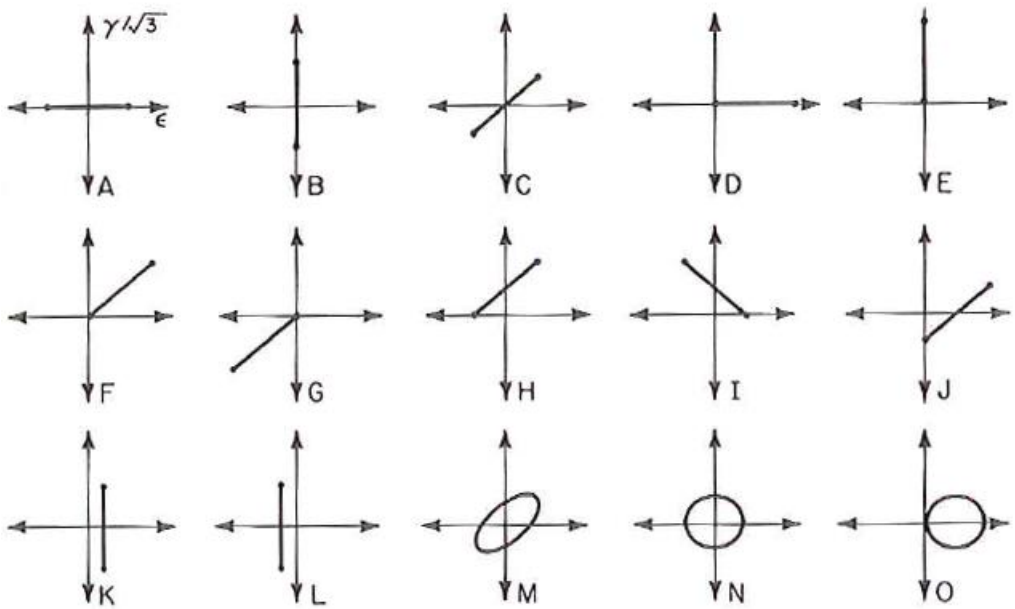

Figure 2. Loading paths simulated (taken from Socie et al., 1989).

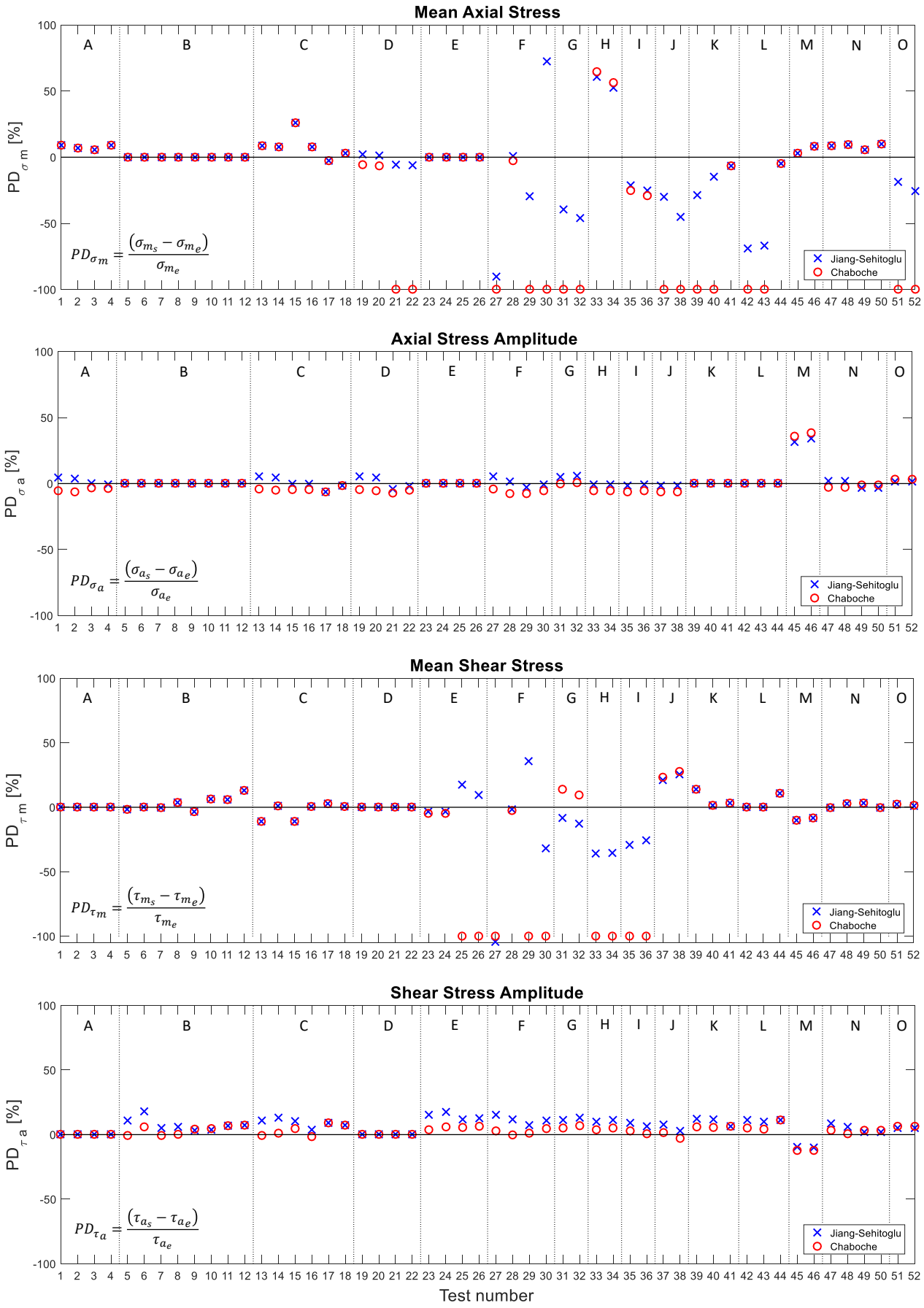

Figure 3. Comparison between experimental and simulated stresses, considering both the J-S and Chaboche models.

Unlike the Chaboche model, the Jiang-Sehitoglu model predicted non-null values of mean stresses at half-life for some specific cases. Hence, the J-S model was more effective in describing the mean stress behavior. For most cases, percentage differences for axial and shear mean stresses ranged from -45 to 60% and -35 to 35%, respectively, for the J-S model, as shown in Figure 3. On the other hand, the respective percentage differences ranged from -100 to 65% and -100 to 30% for the Chaboche model. Some points outside the curve are justified because there is no stress replicability in some cases, as seen in Path F. In others, mean axial compressive loads were observed when the prescribed mean axial strain was null, as seen in Path H. None of the models was effective in perceiving these specific situations. The simulated alternate stresses were very similar to the experimental ones, considering both the J-S and the Chaboche models. Therefore, the percentage differences for these stresses were also minimal for the two plasticity models considered, ranging from -5 to 30% and -10 to 15% for axial and shear alternate stresses, respectively.

The evolution of mean stresses with the loading cycles, as well as the J-S model predictions, are shown in Figure 4 for paths K and L (Fatemi and Kurath, 1988). These loading conditions are characterized by a fully reversed torsional loading applied with a constant tractive (path K) or compressive (path L) load. Figure 4 displays the two conditions considered for paths K (Test 40 and 41) and L (Test 43 and 44) for both experimental and simulated stresses. The J-S model was successful in describing the mean stress evolution of tests with higher absolute values of mean axial strain, represented by tests 41 and 44. At these stress levels, little plasticity is expected after the first cycles. As the phenomenon of mean stress relaxation involves plastic deformations, the mean stress evolution is not observed either experimentally in the simulations. In this case, the maximum percentage difference between the experimental and simulated stresses was around 10%. Tests 40 and 43, with lower mean axial strain, had a 70% discrepancy between simulated and experimental stresses and were not well described by the J-S model. Despite this, it is observed that the simulated mean stress values of test 40 appear to converge to the experimental ones at the end of the fatigue life.

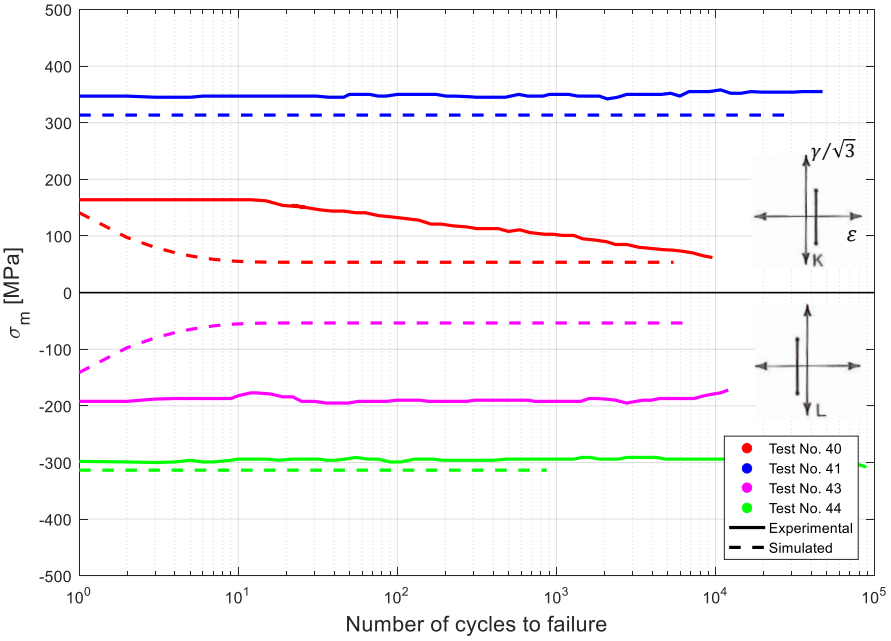

Figure 4. Comparison between experimental and simulated mean stress evolution for fully reversed torsional loading applied with a constant tractive (path K) and compressive (path L) load. Data from Fatemi and Kurath (1988).

Considering the failure mechanism of Inconel 718, fatigue life was estimated based on the Fatemi-Socie model, as previously stated. A cumulative damage approach was used for life estimation to consider the mean stress relaxation effect. Thus, the damage generated by the higher stress levels that occur before relaxation can now be accounted for in the life estimation. This extra damage is neglected when considering only the half-life mean stress for performing the calculations. Note that the plane at which the maximum fatigue parameter is observed depends on the mean stress value. Consequently, this plane can change during the time due to the mean stress relaxation. To consider this effect, the fatigue parameter and damage increment were calculated for all planes in each loading cycle, following Eqs. (7) and (8). The calculation of the cumulative damage at each plane was carried out by Eq. (9). The plane whose total damage first reached the unit value was considered the critical plane, and the loading cycle associated with this situation represents the fatigue life.

The F-S parameter was calculated using hysteresis loops from both the Chaboche and J-S models to assess the influence of mean stress relaxation in life estimations. Figure 5 presents the evolution of the damage increment and the total damage of paths C and J, considering a stress-strain response simulated with the J-S and the Chaboche model. Experimentally, path C has no mean stress relaxation, contrary to what happens with path J. As expected, the damage

evolution simulation of path C was the same considering both the J-S and the Chaboche model. However, this scenario was not repeated for path J: Greater damage was observed in the simulations made with the J-S model, justified by the presence of non-null mean stress after reaching the stabilized stress-strain behavior. Nevertheless, the results shown in Table 2 suggest that this difference between the cyclic plasticity models does not significantly influence fatigue life estimations. This is justified by the fact that most of the analyzed cases either have null mean stress or present total mean stress relaxation. As expected, exceptions occurred precisely in the loading paths where the mean stress was different from zero, as seen in Paths O, K, J, F, and D. Even so, the difference between the lives estimated by both models was minimal, with the largest discrepancy in results being equal to 20%, observed in path O. One possible explanation for this result is the relatively small influence of mean stress relaxation on the evolution of the maximum normal stress. The FS parameter considers the maximum normal stress, composed of the mean stress term and the alternate stress term. Since the alternate stress is significatively greater than the mean stress (smallest absolute difference is 475 MPa, observed in path J), the FS parameter yields similar life estimates for both models even when total relaxation is not observed. As a consequence, life estimates were within a factor of 2 boundaries using both models, as shown in Figure 6.

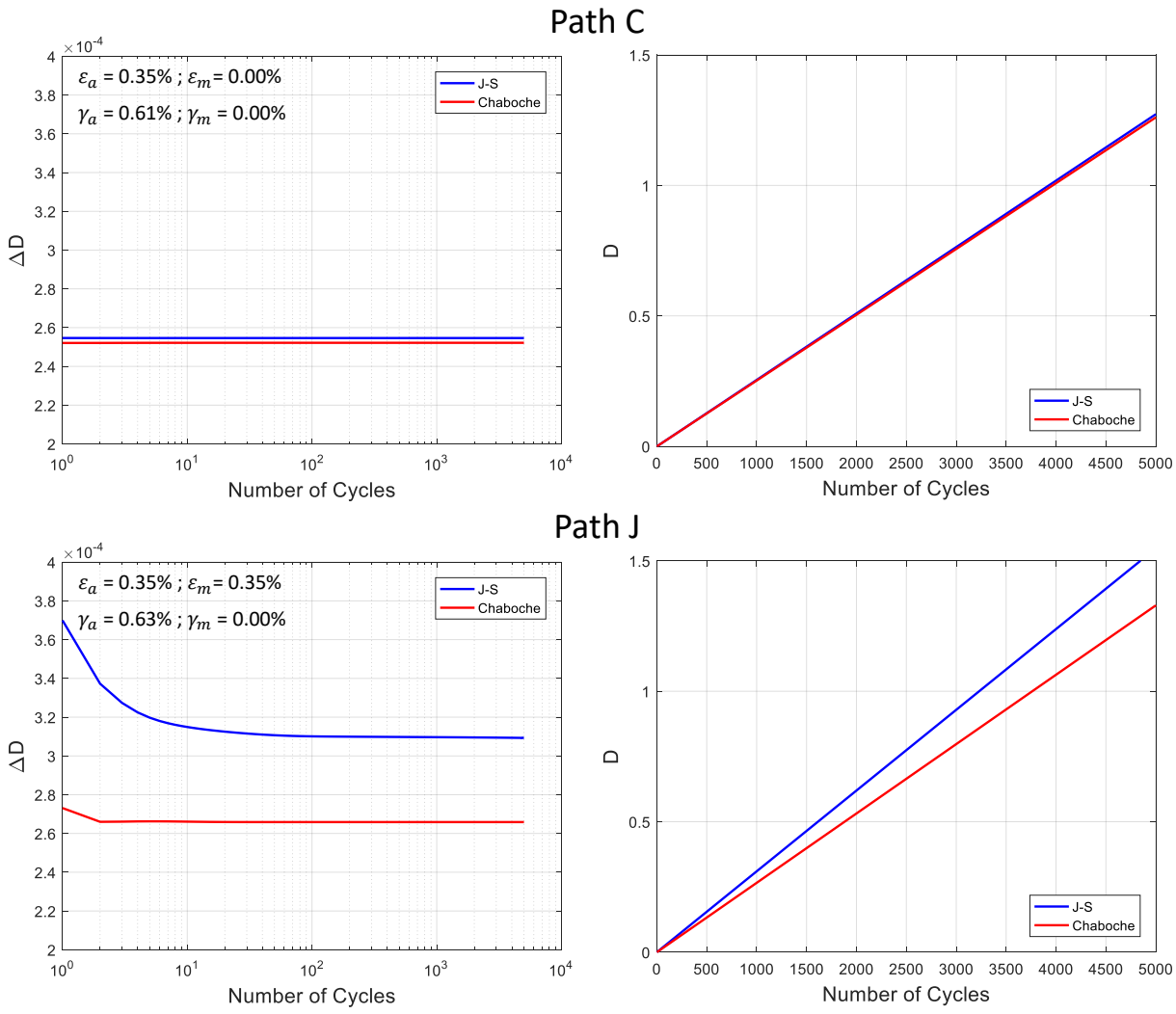

Figure 5. Damage evolution of Paths C and J.

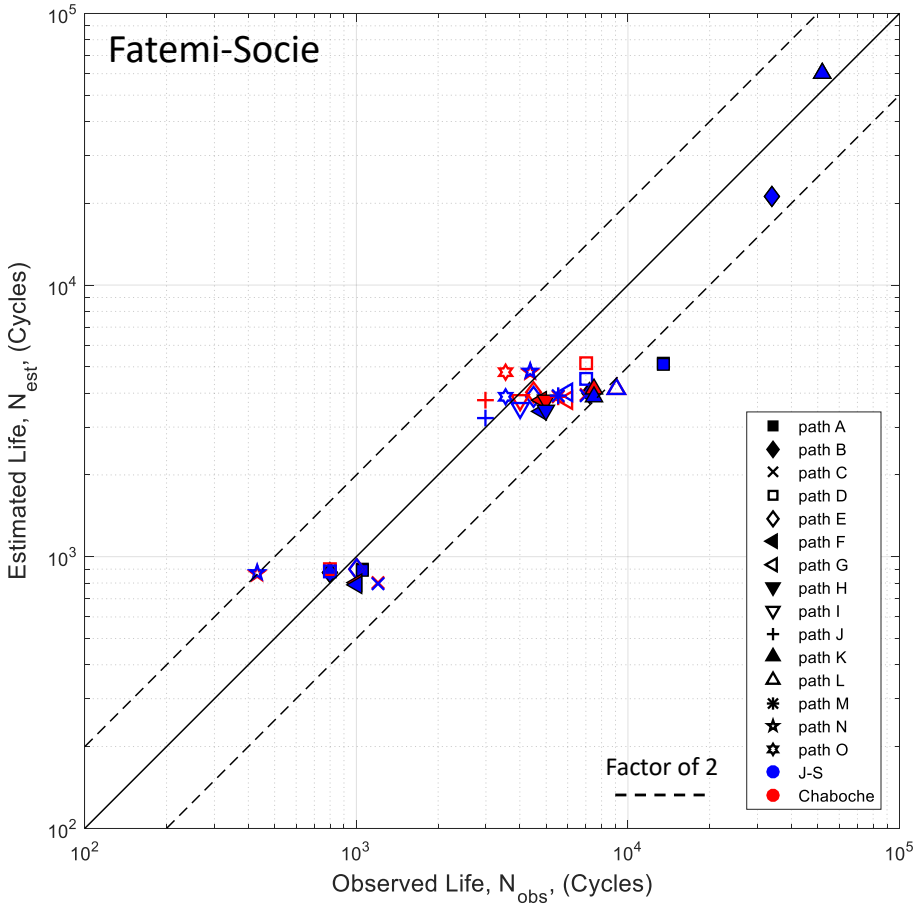

Figure 6. Inconel 718 experimental vs estimated life obtained for the FS criterion using hysteresis loops from the Chaboche and Jiang-Sehitoglu models.

5. CONCLUSIONS

In this work, the influence of the mean stress relaxation on fatigue life estimations of Inconel 718 at room temperature was investigated. In addition, the capability of the cyclic plasticity models proposed by Chaboche and Jiang and Sehitoglu to capture this phenomenon was also addressed. For the axial-torsional data available in the literature, fatigue life estimates were obtained using the Fatemi and Socie criterion for both cyclic plasticity models. The main findings are summarized as follows:

1) The results suggest that the Jiang-Sehitoglu model correctly described situations where the half-life mean stresses assumed non-null values. For most cases, the percentage differences for axial and shear mean stresses ranged from -45 to 60% and -35 to 35%, respectively. For the Chaboche model, the respective differences ranged from -100 to 65% and -100 to 30%. Furthermore, both the J-S and the Chaboche models succeed in simulating conditions where null half-life mean stresses were observed.
2) Lives estimates were similar for both models for all loading conditions, probably due to the high levels of alternate stresses observed, capable of canceling any mean stress effect. The Fatemi-Socie parameter could estimate fatigue life within a factor-of-two boundaries for all loading conditions, regardless of the cyclic plasticity model used to generate the stress-strain response.

6. ACKNOWLEDGEMENTS

Fábio Castro would like to thank the support from the National Council for Scientific and Technological Development – CNPq (contract 307330/2019-2).

7. REFERENCES

Armstrong, P., Frederick, C., 1966. A Mathematical Representation of the Multiaxial Bauschinger Effect, vol. 731.
Chaboche, J.L., 1986. “Time-independent constitutive theories for cyclic plasticity”. *Int. J. Plast. 2*, 149–188.

Chaboche, J.L., Van, K.D., Cordier, G., 1979. “Modelization of the strain memory effect on the cyclic hardening of 316 stainless steel”. *Transactions of the International Conference on Structural Mechanics in Reactor Technology L*.

Fatemi, A., Kurath, P., 1988. “Multiaxial fatigue life predictions under the influence of mean-stresses”. *Transactions of the ASME*, Vol. 110, pp. 380–388.

Fatemi, A., Socie, D., 1988. “A critical plane approach to multiaxial fatigue damage including out-of-phase loading”. *Fatigue Fract. Engng Mater. Struct.*, Vol 11, No. 3, pp 149–165.

Jiang, Y., Sehitoglu, H., 1996a. “Modeling of cyclic ratchetting plasticity, Part I - Development of constitutive relations”. *Transactions of the ASME*, Vol. 63, pp. 720–725.

Jiang, Y., Sehitoglu, H., 1996b. “Modeling of cyclic ratchetting plasticity, Part II – Comparison of model simulations with experiments”. *Transactions of the ASME*, Vol. 63, pp. 726–733.

Socie, D., Shield, T.W., 1984. “Mean stress effects in biaxial fatigue of Inconel 718”. *Journal of Engineering Materials and Technology*, Vol. 106, pp. 227–232.

Socie, D., Waill, L., Dittmer, D., 1985. “Biaxial fatigue of Inconel 718 including mean stress effects”. *ASTM Special Technical Publication*, STP 853, pp. 463–481.

Socie, D., 1987. “Multiaxial fatigue damage models”. *Journal of Engineering Materials and Technology*, Vol. 109, pp. 293–298.

Socie, D., Kurath, P., and Koch, J., 1989. “A multiaxial fatigue damage parameter”. *Biaxial and Multiaxial Fatigue*, EGF 3, pp. 535–550

Socie, D., Marquis, G.B., 2000. “Multiaxial fatigue”. *SAE International*.

8. RESPONSIBILITY NOTICE

The authors are the only responsible for the printed material included in this paper.